

Static and fatigue investigation of second generation steel-free bridge decks

Chad Klowak ^{a,*}, Amjad Memon ^b, Aftab Mufti ^a

^a *ISIS Canada Research Network, University of Manitoba, A250 96 Dafoe Road, Winnipeg, Canada MB R3T 2N2*

^b *Wardrop Engineering, 1400-410 22nd Street East, Saskatoon, Canada SK S7K 5T6*

Available online 11 September 2006

Abstract

This paper outlines the static and fatigue behavior of two different cast-in-place second generation steel-free bridge decks. Although cast monolithically, the first bridge deck was divided into three segments. The first segment was reinforced according to conventional design with steel reinforcement. The other two segments were both steel-free designs with internal crack control grids, one comprised of CFRP, and the other with GFRP. The hybrid CFRP/GFRP and steel strap design is called the second generation of the steel-free concrete bridge deck. The hybrid system reduces the development of longitudinal crack width and eliminates corrosion in the deck. All three segments were tested under a 25 ton and 60 ton cyclic load to investigate fatigue behavior. The second bridge deck is comprised of an internal panel and two cantilevers and incorporates a complete civionics system [Klowak C, Mufti A. Implementation of civionics in a second generation steel-free bridge deck. In: Proceedings of the 33rd annual general conference of the Canadian Society for Civil Engineering. Toronto, Ont., June 2–4, 2005]. The static test outlined in this paper is useful in the development of fatigue theory derived from the fatigue testing of the first bridge deck.

© 2006 Elsevier Ltd. All rights reserved.

Keywords: Steel-free; Fatigue testing; Static testing; Glass fibre reinforced polymer; Carbon reinforced polymer; Civionics

1. Introduction

The decline in North American infrastructure has never been more prevalent than it is today. In particular, the highway system and its bridges have been adversely affected by age and weathering over the past two decades. The majority of highway bridges have reinforced concrete decks supported on steel or concrete girders. Over time, the weather has taken its toll on these reinforced concrete decks. Rainwater and de-icing chemicals applied to roadway surfaces during the winter months have seeped through many concrete decks and caused corrosion of the internal reinforcing steel and deterioration of the concrete bridge decks.

This paper describes the static and fatigue behavior of two different cast-in-place second generation steel-free

bridge decks. Although cast monolithically, the first bridge deck was divided into three segments (A–C). Segment A was reinforced according to conventional design with steel reinforcement. Segment B and C were reinforced internally with a CFRP crack control grid and a GFRP crack control grid, respectively, and externally with steel straps. The hybrid CFRP/GFRP and steel strap design is called a second generation steel-free concrete bridge deck. All three segments were designed with an almost equal ultimate capacity so that a direct comparison between the segments under fatigue loading conditions could be made. A performance comparison of all three segments for the first bridge deck under a 25 ton and 60 ton cyclic load is reported in this paper. The paper also outlines the details of a larger second generation steel-free bridge deck and briefly outlines some of the preliminary results from the internal panel static test. The static behavior of the bridge deck plays an important role in understanding the fatigue theory developed from the series of fatigue tests outlined in this paper.

* Corresponding author. Tel.: +1 204 474 6967; fax: +1 204 474 7519.
E-mail address: klowaks@ms.umanitoba.ca (C. Klowak).

The deck will also be subjected to a series of fatigue tests that will help confirm fatigue theory.

2. Fatigue testing

2.1. Bridge deck details

The overall dimensions of the full-scale bridge deck were 3000 mm in width and 9000 mm in length with a deck thickness of 175 mm. It was comprised of an internal panel and two cantilevers. The spacing of the girders was 2000 mm center to center. Although cast monolithically, the slab was conceptually divided into three segments (Fig. 1). Segment A of the bridge deck slab was reinforced

with steel reinforcement and was designed using the empirical design method according to the CHBDC (2000) [2]. It contained two layers of steel reinforcement with 15M bars spaced at 300 mm in both directions in each layer, providing a total reinforcement ratio of 2.08% and 0.52% in the transverse and longitudinal directions for both layers (Fig. 1).

Segment B of the bridge deck was a steel-free/CFRP hybrid design, reinforced with a CFRP crack control grid internally and externally with steel straps. The CFRP crack control grid was comprised of #10 CFRP bars spaced at 200 mm in the transverse direction and 300 mm in the longitudinal direction providing a reinforcing ratio of 0.19% and 0.13% in the transverse and longitudinal

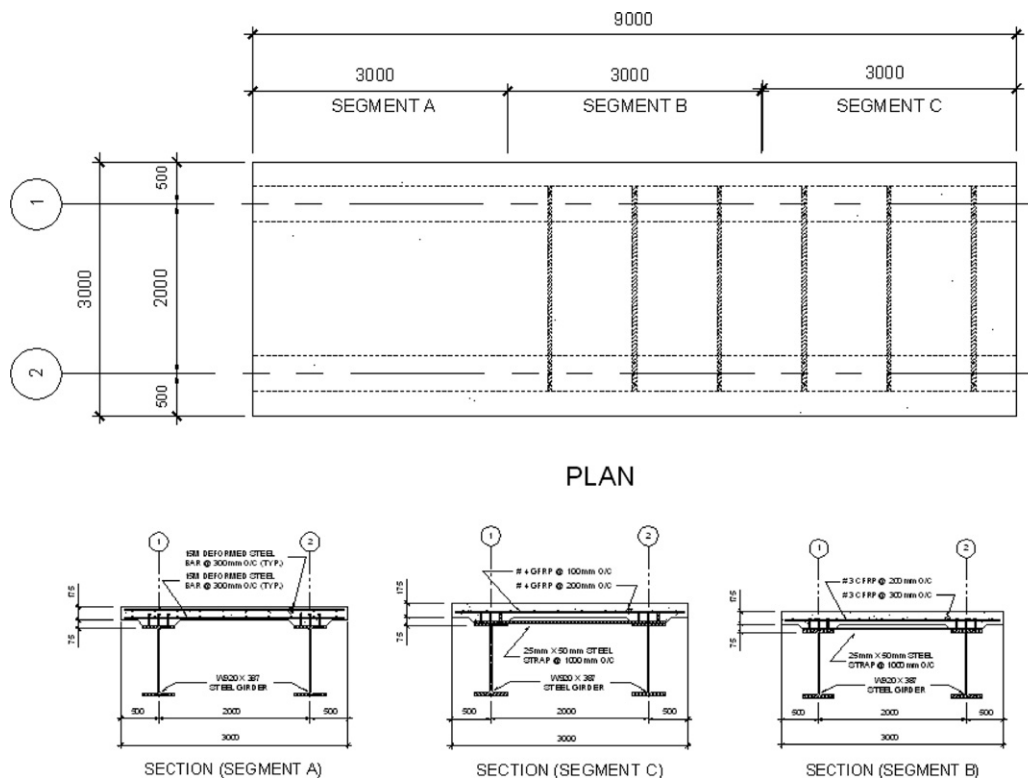


Fig. 1. Bridge deck reinforcement details.

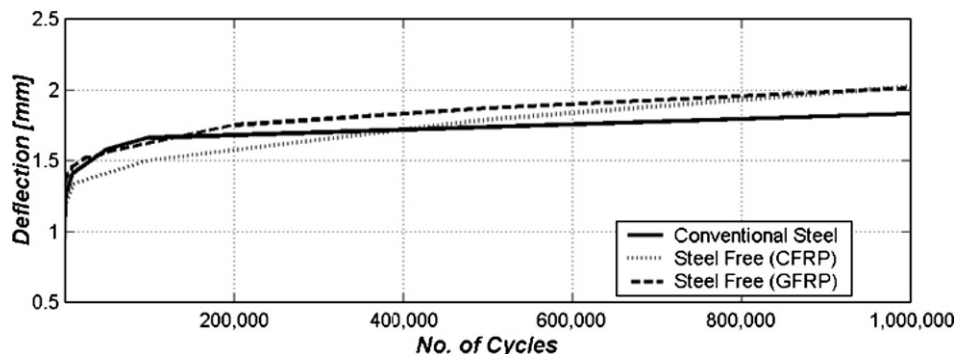


Fig. 2. Plot of deflection versus number of cycles at 25 ton.

directions, respectively [3]. A steel strap having dimensions 25 mm by 38 mm spaced at 1000 mm in the transverse direction provided a reinforcing ratio of 0.55% (Fig. 1).

Segment C of the bridge deck slab was a steel-free/GFRP hybrid design, reinforced with a GFRP crack control grid internally and external steel straps. The GFRP crack control grid was comprised of #13 GFRP bars spaced at 150 mm in the transverse direction and 200 mm in the longitudinal direction providing a reinforcing ratio of 0.48% and 0.36% in the transverse and longitudinal directions respectively. A steel strap having dimensions 25 mm by 38 mm spaced at 1000 mm in the transverse direction provided a reinforcing ratio of 0.55% (Fig. 1).

2.2. Fatigue test results

2.2.1. Test results for 25 ton (245 kN) cyclic loading

Test results show that for a 25 ton or 245 kN cyclic loading, which was chosen to represent service loads, all three segments of the bridge deck completed one million cycles without significant damage [4]. Vertical deflection of all three segments of the bridge deck were measured by displacement transducers and the maximum deflection was found to be approximately 2 mm after completing one million cycles (Fig. 2).

In order to measure the internal and external response of each segment of the bridge deck, strain gauges were

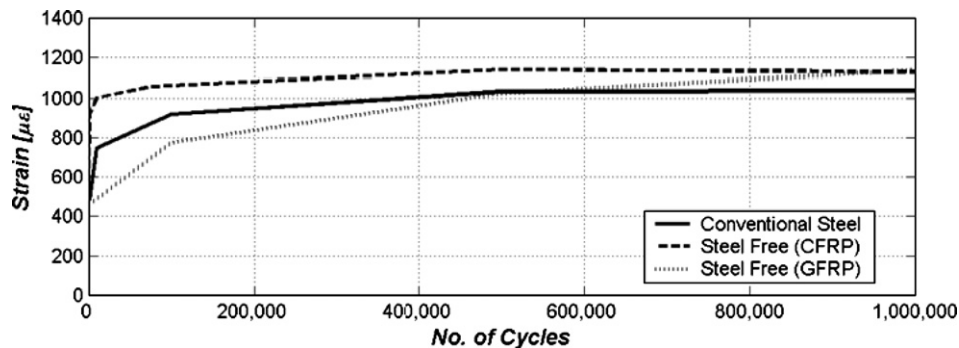


Fig. 3. Plot of reinforcement strain versus number of cycles at 25 ton.

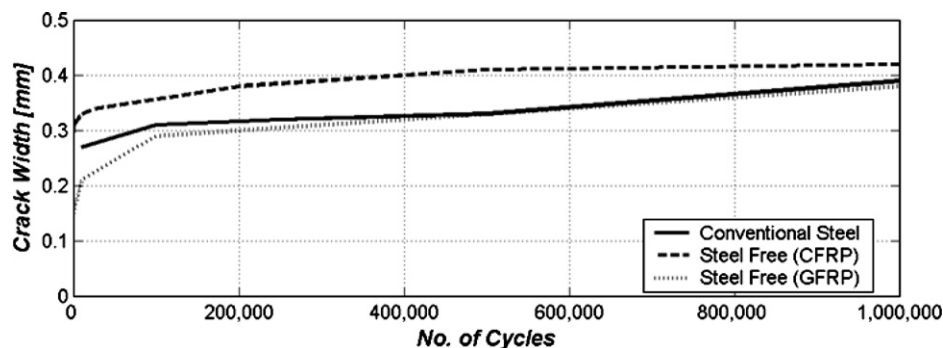


Fig. 4. Plot of crack longitudinal crack width versus number of cycles.

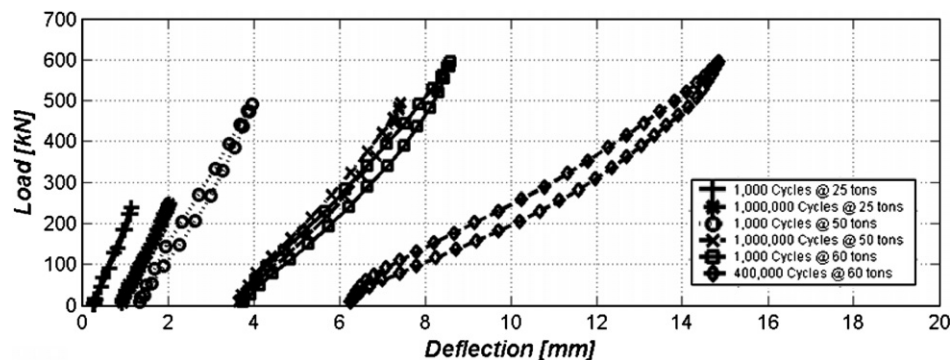


Fig. 5. Plot of load versus deflection for steel-free deck with internal GFRP reinforcement.

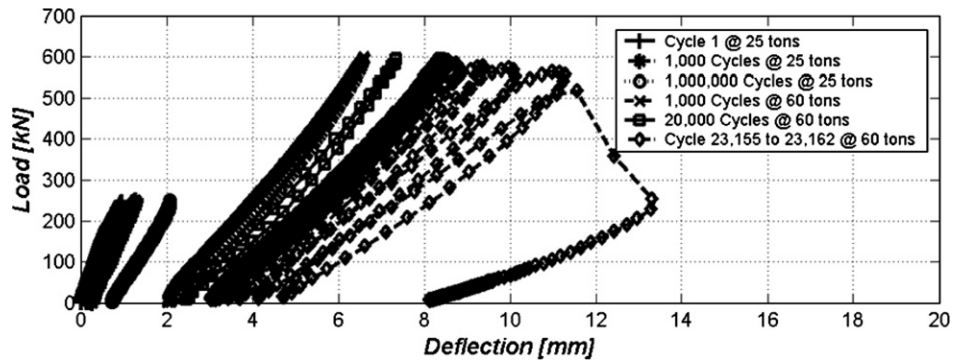


Fig. 6. Plot of load versus deflection for deck with conventional steel reinforcement.

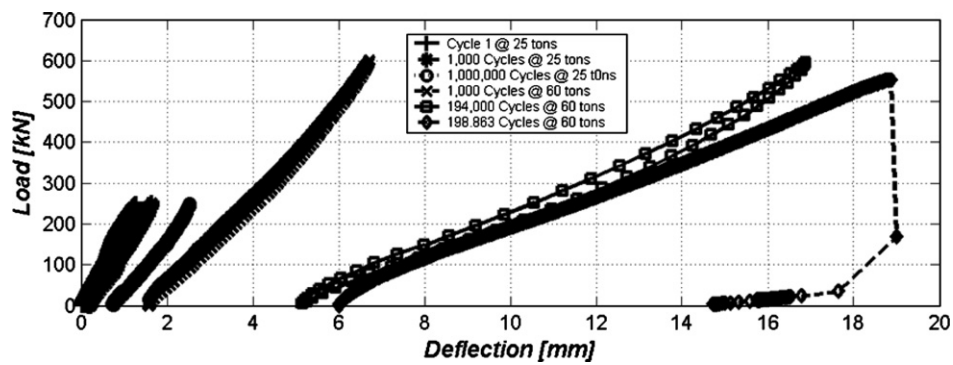


Fig. 7. Plot of load versus deflection for steel-free deck with internal CFRP reinforcement.

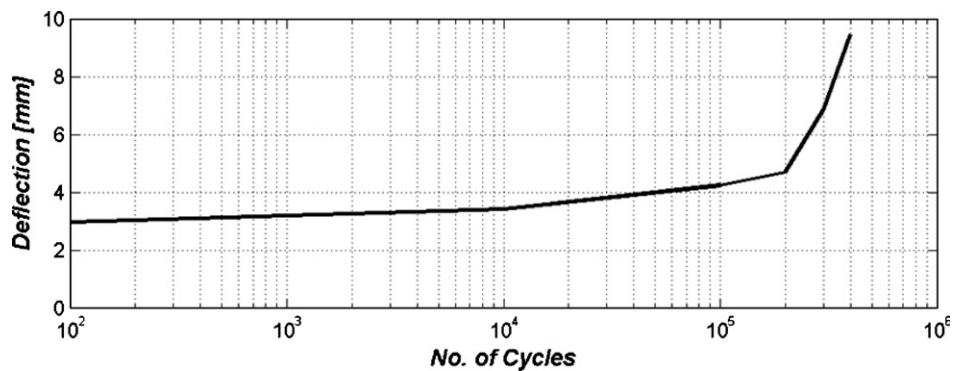


Fig. 8. Net Deflection of steel-free deck with internal GFRP reinforcement at 60 ton.

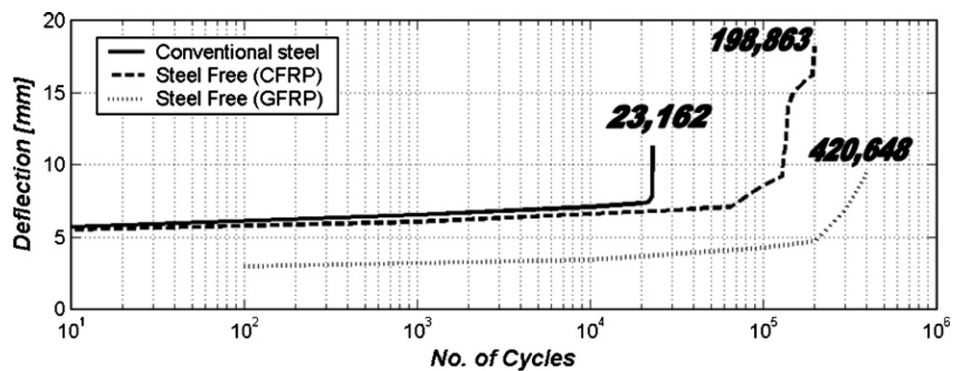


Fig. 9. Plot of deflection versus number of cycles at 60 ton.

installed on some of the steel, CFRP and GFRP bars. Maximum response was measured under the applied load in the transverse direction (Fig. 3). All strain values are lower than 1200 micro-strain, which meant that serviceability criteria were satisfied. The serviceability limit for either CFRP or GFRP is 2000 micro-strain [5]. Therefore, the test results suggest that there could be a reduction of up to 40% in the area of CFRP or GFRP.

In order to determine the effect of CFRP or GFRP crack control grids on the growth of crack width, a longitudinal crack was measured with an increasing number of cycles under the applied load (Fig. 4). It can be seen that the maximum crack width for all three segments was approximately 0.4 mm, after completing one million cycles for a 25 ton or 245 kN cyclic load. The ACI Committee 440 (2001) reported that, for steel reinforced structures, the allowable crack width limits are 0.3 mm for exterior exposure [6]. However, because FRP rods are corrosion resistant, the maximum crack width limitation can be relaxed. Nevertheless, excessive crack width is undesirable aesthetically and it contributes to the damage or deterioration of structural concrete.

2.2.2. Results for 60 ton (588 kN) cyclic loading

Segment C was the first section of the bridge to be tested at a load level above 25 ton. After completing 1,000,000 cycles without significant damage the load level was increased to 50 ton or 490 kN. After achieving an additional 1,000,000 cycles without failure the load level was then increased to 60 ton or 588 kN causing Segment C to fail at 420,648 cycles. The deflection behavior of Segment C is plotted against an increasing number of cycles in Fig. 5.

Due to the fact that Segment C did not fail at a load level of 50 ton or 490 kN after completing 1,000,000 cycles it was determined that Segment A and Segment B would be subjected to 60 ton or 588 kN immediately after completing 1,000,000 cycles at 25 ton or 245 kN. Test results indicate that deck Segment A and deck Segment B failed in punching shear at 23,162 cycles and 198,863 cycles, respectively, when subjected to a cyclic load of 60 ton or 588 kN. The deflection behavior for deck Segment A and deck Segment B are shown in Figs. 6 and 7. The figures show

that the deflection of both Segment A and Segment B has significantly increased when subjected to 60 ton or 588 kN load levels.

Bridge deck Segment C was tested under a 50 ton or 490 kN load level and Segment A and Segment B were not. Therefore, in order to make a comparison among all three segments, the net deflection behavior for deck Segment C at 50 ton or 490 kN was deducted or subtracted from the net deflection behavior recorded under the 60 ton or 588 kN load level (Fig. 8). Figs. 9 and 10 illustrate the deflection and crack width behavior for all three bridge deck segments under the 60 ton or 588 kN load level. The results show that deck Segment A failed in punching shear approximately twenty times as fast as deck Segment C and deck Segment B failed in punching shear approximately twice as fast a deck Segment C.

3. Static investigation

3.1. Bridge deck details

Construction of a full-scale second generation steel-free bridge deck including the implementation of a complete civionics structural health monitoring system was completed in March 2004 [1]. The bridge deck is a slab on steel girder superstructure comprised of a continuous deck supported by two steel girders. It measures 9000 mm in length and 5000 mm in width. The thickness of the deck is 200 mm, and it contains haunches over the girders that measure 75 mm in depth (Fig. 11).

The spacing of the girders is 2500 mm center to center. The internal panel is a second generation steel-free design and utilizes 25 mm by 50 mm steel straps spaced at 1200 mm center to center. A bottom mat of GFRP is incorporated in the internal panel to control cracking at service loads. The transverse and longitudinal crack control reinforcement consists of #10 Pultrall V-Rod spaced at 200 mm and 600 mm center to center, respectively. A GFRP crack control grid was chosen for the bridge deck because GFRP had the highest fatigue resistance when compared to CFRP and conventional steel reinforcement [3]. The top mat of reinforcement required for the

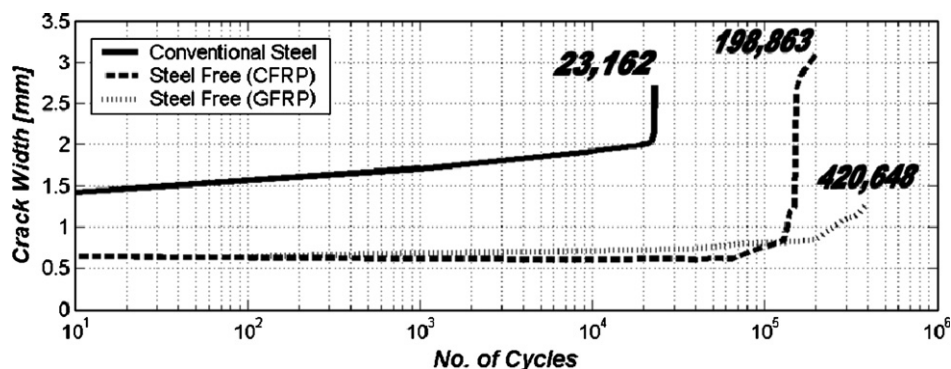


Fig. 10. Plot of crack width versus number of cycles at 60 ton.

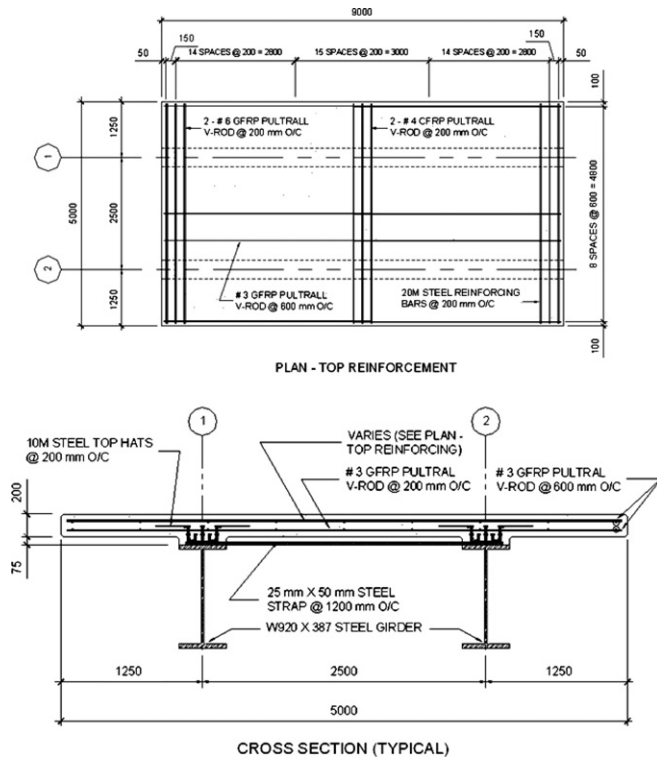


Fig. 11. Bridge deck details.

cantilevers is divided into three 3000 mm sections in order to provide a comparison between GFRP, CFRP, and steel when the deck is subjected to destructive fatigue testing. Each of the three sections was designed to have the same nominal moment capacity. The three sections use #10 GFRP Pultrall V-Rod for longitudinal reinforcement spaced at 600 mm center to center. The transverse negative moment reinforcement uses two #19 GFRP and two #13 CFRP Pultrall V-Rod spaced at 200 mm center to center in the steel-free portion of the bridge deck, and one 20M steel reinforcing bar spaced at 200 mm center to center for the section of the deck with conventional cantilever reinforcement. Occasionally on bridge deck rehabilitation projects, existing studs on the steel supporting girders have insufficient length to fully ensure composite action between the deck and the girders. For such cases it may be more

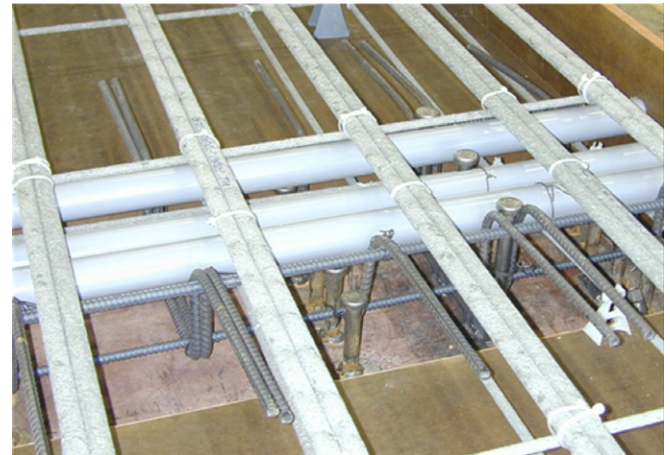


Fig. 12. Steel top-hat reinforcement.

economical to extend the depth of stud penetration into the deck through the use of addition steel reinforcement called top-hats, rather than completely removing existing studs and replacing them with new ones. As a means of investigating such design alternatives, short steel studs were welded to the girders and additional top-hat reinforcement comprised of 10 M steel bars at 200 mm center to center with alternate top-hats doubled up were placed in the haunches over the girders (Fig. 12).

3.2. Internal panel static test results

3.2.1. Mode of failure

The internal panel exhibited a typical punching failure. Failure occurred at an ultimate load of 980 kN. A longitudinal crack was first apparent at a load of 250 kN and developed in length until failure. Radial cracks were visible at a load of 300 kN and continued to move outwards until failure. Punch angles along the north, east, and south axis were approximately 18°, 21°, and 25°, respectively (Fig. 13).

3.2.2. Load deflection behavior

The first test on the bridge deck was conducted on December 15, 2004. The static ultimate capacity of the deck when loaded monotonically until failure was 980 kN, and

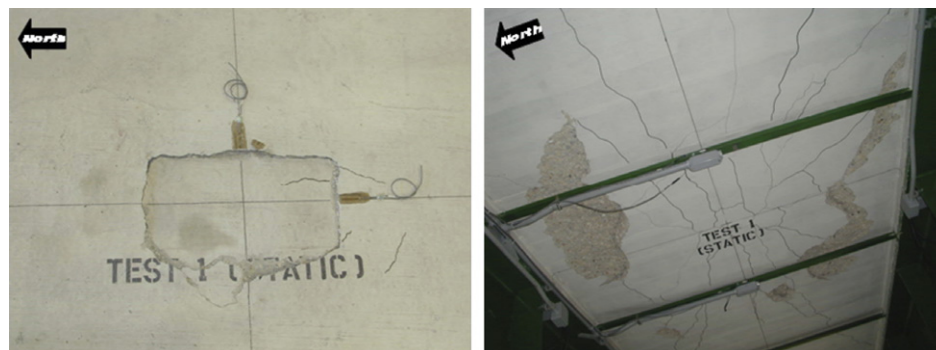


Fig. 13. Top and bottom view of internal panel punch cones.

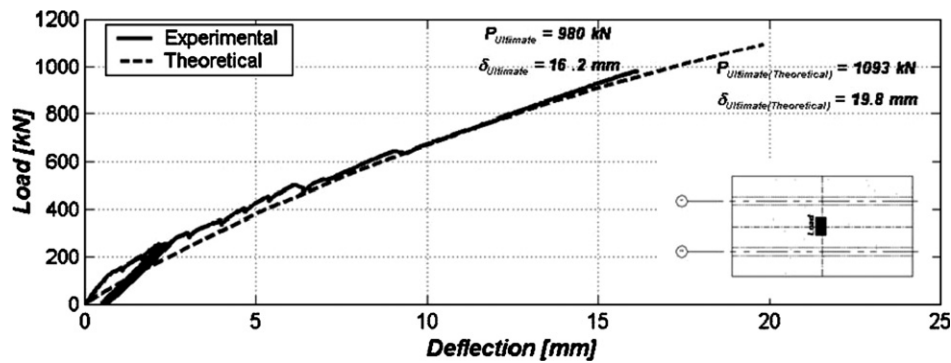


Fig. 14. Plot of load versus deflection for internal panel static test.

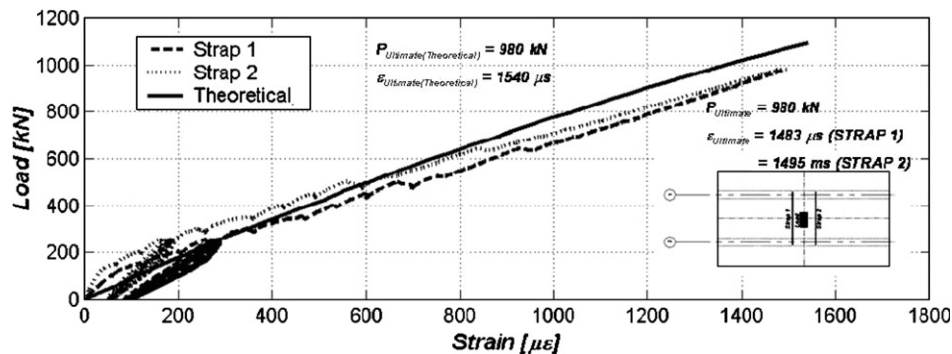


Fig. 15. Plot of load versus strain of steel straps for internal panel static test.

the maximum deflection at the time of punching failure was recorded to be 16.2 mm. The theoretical ultimate load and deflection determined using a computer program called PUNCH were 1093 kN and 19.8 mm, respectively [7]. Klowak et al. were able to successfully predict the ultimate load of the deck slab to within 11.5%. However, the predicted maximum deflection was 3.6 mm or 22.2% greater than the experimental deflection measured during the test (Fig. 14).

3.2.3. Load strain behavior

The strain in the straps at failure was determined to be 1483 micro-strain and 1495 micro-strain in straps one and two, respectively (Fig. 15). The strains in the straps

were approximately 74% of their yielding strength at the time of failure. The PUNCH Program, was used to determine the theoretical strains in the straps. The theoretical ultimate strain in the straps was found to be 1540 micro-strain, approximately 3.4% greater than that observed during the test.

4. Static and fatigue relationship

Due to the limitations of performing full-scale tests in a laboratory, the bridge deck outlined in Section 2 of this paper was only subjected to cyclic loading conditions. In the absence of static loading tests, all three segments of the deck were analyzed using the PUNCH Program. The

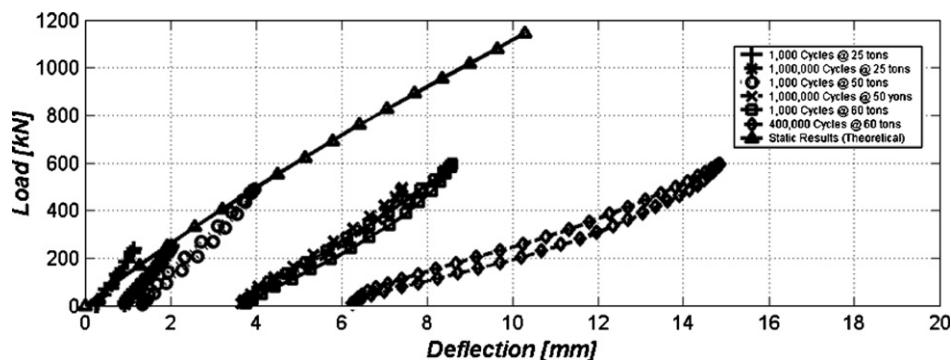


Fig. 16. Plot of static (theoretical) and fatigue load versus deflection for steel-free deck with internal GFRP reinforcement.

ultimate capacity of the steel-free deck with internal GFRP reinforcement was determined to be 1145 kN or 117 ton and the static load deflection behavior predicted by the program is shown in Fig. 16. This figure illustrates how the deflection under cyclic loading conditions is much higher than that predicted by the static monotonic loading conditions. Cyclic loading of variable amplitudes results in cumulative damage that reduces the capacity of the deck for further load distribution. Similar results were found by Hongseob Oh et al. [8]. In order to verify deflections under monotonic and cyclic loading conditions, the bridge deck outlined in Section 3 of the paper was constructed; however, fatigue data for this bridge deck is not yet available.

Based on the limited fatigue tests outlined in Section 2 of this paper, a method for estimating the fatigue strength has been suggested by Memon [9]. According to this method, the number of cycles to fatigue failure can be predicted by

$$n = 10^5 \sqrt{\left(\frac{1}{P/P_u}\right)^{-1}} \quad (1)$$

where, n is the number of cycles to failure, P is the magnitude of the applied load, and P_u is the ultimate static capacity of the bridge deck. Further refinement is expected as additional fatigue data becomes available.

5. Conclusions

A bridge deck containing an internal CFRP or GFRP crack control grid and external steel straps prevents the growth of longitudinal crack widths and eliminates corrosion in the deck. Experimental results suggest that the area of CFRP or GFRP can be reduced by up to 40% [9]. Experimental results also indicate that fatigue damage induced under a 25 ton cyclic load is within permissible limits and that all three bridge deck segments were subjected to one million cycles under a 25-ton cyclic load without significant damage. The results show that all three segments of the bridge deck failed in fatigue under a 60 ton or 588 kN cyclic load. Conventional steel reinforcement failed after completing 23,162 cycles. The steel-free deck with CFRP internal reinforcement failed after completing 198,863 cycles and the steel-free deck with internal GFRP reinforcement failed after completing 420,648 cycles at 60 ton. The second generation steel-free bridge deck with external steel straps and internal GFRP reinforcement for crack control provides the best fatigue performance and

is an efficient, economical, and corrosion free system for bridge deck superstructures [10]. The ability to predict ultimate loads to within an accuracy of 11.5% indicates that the static behavior of a second generation steel-free bridge deck has been well established.

Acknowledgements

The authors would like to gratefully acknowledge the financial support provide by the ISIS Canada Research Network. In addition, they would like to thank Specialty Construction Products Ltd., Pultrall Inc., PCL Constructors Canada Ltd., and Hansch Ernst Construction Ltd. for providing the materials necessary to construct the bridge decks. The authors would also like to acknowledge the contributions of Ms. Evangeline Rivera, Mr. Moray McVey, and Mr. Grant Whiteside for their technical assistance throughout these two projects.

References

- [1] Klowak C, Mufti A. Implementation of civionics in a second generation steel-free bridge deck. In: Proceedings of the 33rd annual general conference of the Canadian Society for Civil Engineering. Toronto, Ont., June 2–4, 2005.
- [2] Canadian highway bridge design code. Canadian Standards Association International. Toronto, Ont., Canada, 2000.
- [3] Memon AH, Mufti AA, Bakht B. Crack control with GFRP bars in steel-free concrete deck slab. In: Proceedings of the 2003 Canadian Society for Civil Engineering Annual Conference. Moncton, New Brunswick, Canada, 2004.
- [4] Mufti AA, Memon AH, Klowak C. Study of static and fatigue behaviour of second generation bridge decks. In: Proceedings of the international workshop on innovative bridge deck technologies. Winnipeg, MB, 2005. p. 49–65.
- [5] Rizkalla S, Mufti AA. “Reinforcing Concrete Structures with Fibre Reinforced Polymers”, Design Manual #3, ISIS Canada Research Network. Winnipeg, Manitoba, Canada, 2001.
- [6] ACI 440.1R-01. Guide for the design and construction of concrete reinforced with FRP bars. Reported by ACI Committee 440, USA, 2001.
- [7] Newhook JP, Mufti AA. Punch program user manual Nova Scotia CAD/CAM Centre. Halifax, Nova Scotia: Dalhousie University; 1998.
- [8] Oh H, Sim J, Meyer C. Fatigue life of damaged bridge deck panels strengthened with carbon fiber sheets. *ACI Struct J* 2005;102(1): 85–92.
- [9] Memon AH. Thesis—Fatigue behavior of steel-free concrete bridge deck slabs under cyclic loading. Winnipeg, Manitoba, Canada, 2005.
- [10] Memon AH, Mufti AA. Fatigue behaviour of second generation steel-free concrete bridge deck slab. In: Proceedings of the second international conference on FRP composites in civil engineering (CICE 2004). Adelaide, Australia, 2004.